Textures and Microstructures, 1990, Vol. 12, pp. 125–140
Reprints available directly from the publisher.
Photocopying permitted by license only

INTERLABORATORIES TESTS OF TEXTURES OF ZIRCALOY-4 TUBES. PART 1: POLE FIGURE MEASUREMENTS AND CALCULATION OF KEARNS COEFFICIENTS

J. L. BARON,[1] C. ESLING,[2] J. L. FERON,[3] D. GEX,[4] J. L. GLIMOIS,[3] R. GUILLEN,[3] M. HUMBERT,[2] P. LEMOINE,[1] J. LEPAPE,[5] J. P. MARDON,[6] A. THIL[2] and G. UNY[7]

[1]D. Tech/SRMA, CEN SACLAY, F-91191 Gif sur Yvette Cedex, [2]LM2P, Faculté des Sciences, Ile du Saulcy, F-57045 Metz Cedex, [3]LAMM, IUT Saint-Nazaire, BP 420, F-44606 Saint-Nazaire, [4] Centre de Recherche d'Ugine-Cezus, F-73400 Ugine, [5]ZIRCOTUBE, Usine de Paimboeuf, F-44560 Paimboeuf, [6]FRAGEMA, 10 rue J. Récamier, F-60996 Lyon, [7]SEM-LECM, CENG, F-38041 Grenoble Cedex.

(Received December 8, 1988; in final form February 16, 1989)

Interlaboratories tests of textures initiated by ZIRCOTUBE, a manufacturer of zircaloy tubes and FRAGEMA, a designer, have been organized. The study focuses on cladding tubes in the cold worked stress relieved state and on thimble tubes, standard section and reduced section, in the fully annealed state.

The first part of the tests consists in measuring incomplete pole figures in reflection, in drawing the (RD, LD) and (RD, TD) linear sections of the pole figure (00.2) and in calculating the f_R, f_T, f_L Kearns coefficients relative to the pole figure (00.2).

The synthesis of the reports presented by the three industrial teams and by two university teams, which have taken part in the interlaboratories tests, shows that the results are rather clustered, the remaining differences could have been brought about by various preparations of samples and by various adjustments of the measuring devices.

This study will be completed by three-dimensional analyses of texture using programs developed or purchased by the different laboratories (Second part).

KEY WORDS Zircaloy-4, Pole figures, Kearns coefficients.

1. INTRODUCTION

The texture is one of the main characteristics of the polycrystal structures. In many cases it makes it possible to estimate the macroscopic behaviour of the polycrystal, when the one of the monocrystal is known (thermal dilatation, growth under irradiation, elastic, magnetic, plastic properties, etc . . .)

From the mathematical point of view, the texture is presented through the Orientation Density Function (ODF). The means commonly used to calculate the ODF is the integral equation (Bunge, 1982; Bunge and Esling, 1982; Vadon, 1981);

$$P_h(\alpha, \beta) = \frac{1}{2\pi} \int_{y//h} f(g)\, d\gamma \qquad (1)$$

where $P_h(\alpha, \beta)$ represents the distribution of poles $h = (hkl)$ i.e. the Pole Figures (PF). But unfortunately traditional measurements in texture goniometry only provide average values of this pole distribution per solid angle. What is even worse, is the disturbance by a certain number of factors, geometrical factors on the one hand and factors which are inherent to the diffraction on the other hand. The experimenter has to use his knowledge to choose the best measurement conditions in order to minimize the effect of such distorsions (Humbert, 1987).

The comparison of the results obtained by the various laboratories is a basis, which allows each experimenter to improve the quality of the measurements (Lewis *et al.*, 1979). Thus ZIRCOTUBE, which manufactures zircaloy cladding tubes and FRAGEMA, which designs with such products, have organized interlaboratories tests with industrial and university research laboratories. They have access to a texture goniometer and operational texture analysis programs. The program and the specifications of the contract of the interlaboratories tests have been set up. It was decided in close cooperation with the partners that the tests should be performed on three tubular products of zircaloy-4: one cladding tube in a cold worked, stress relieved state and two samples of thimble tubes in a fully annealed state, which were respectively taken from the standard section and the reduced section.

On the other hand, it was agreed that the first part of the study should be devoted to the measurement of four incomplete PFs in reflection until $\alpha_{max} = 75°$, and to the calculation and the drawing of PFs, where the background noise only was corrected, and of PFs, where both the background noise and the defocalisation were corrected. In both cases, they are normalized according to the pseudo-norm technique (Kern and Bergmann, 1978), which presupposes that the integral of the diffracted intensity in the incomplete figure is proportional to the examined solid angle.

This first part comprises the calculation of the Kearns coefficients (Kearns, 1965) of all samples. Table 1 shows the list of the laboratories taking part in the

Table 1 List of laboratories which have presented their results at the final meeting of the first part of the tests

Laboratory	*Participant(s)*
Centre de Recherche d'Ugine- Cezus	D. Gex
Laboratoire d'Application Matériaux-Mécanique LAMM IUT Saint-Nazaire	J. L. Feron J. L. Glimois R. Guillen
Commissariat à l'Energie Atomique SEM-LECM, CEN Grenoble	G. Uny
Laboratoire de Métallurgie des Matériaux Polycristallins LM2P, Université Metz	C. Esling M. Humbert A. Thil
Commissariat à l'Energie Atomique D. Tech/SRMA, CEN Saclay	J. L. Baron P. Lemoine

round-robin and having presented their results in the final meeting, during which a synthesis of the first part of tests has been worked out.

The first part of the study will be followed by a second part where three-dimensional analyses from experimental pole figures will be performed. This final part has to comprise the calculation of Orientation Density Functions, Pole Figures recalculated on the basis of these ODFs and finally the calculation of error coefficients, related to the numerical precision of these analyses. These error coefficients are based on the comparison of the experimental and the recalculated figures.

2. THE SAMPLES

The test-tubes were selected according to a sampling scheme. The organizers have thus chosen three different types of tubular samples listed in Table 2, where t stands for the wall thickness.

The samples were delivered in the form of 50 mm long cylindrical sections with various external diameters (see Table 2) and made thinner by chemical dissolution to a thickness of about 0.1 mm. Several laboratories even asked for rough samples so that they could perform the chemical slimming by themselves. We should therefore point out that the teams worked with samples of the same type (cladding or thimble tubes), but which were unequally prepared to some extent. By this fact, an additional random parameter is introduced in the comparison, the effects of which are difficult to evaluate.

The micrographies which have been performed by ZIRCOTUBE are displayed in Figure 1. Both fully annealed states show approximately equi-axial grains with the average diameter of 8 μm. On the contrary the cold worked stress relieved state shows distorted grains with a width of 4–5 μm in the tangential direction and with a pronounced length (60 to 80 μm) in the axial direction. In the latter case, the marked morphological anisotropy leads to a difficulty in the statistical sampling of the grains. Indeed, when the translation of the sample performs the scanning of the RX beam in the axial (or longitudinal) direction, the number of grains which are involved in the diffraction is about ten times lower than the one of the grains involved in the diffraction, when the scanning is performed in the tangential direction.

Table 2 Tubular Zircaloy-4 samples which were provided to the various laboratories.

No.	*Nature and geometry of the product*	*Final metallurgical state*
1	Cladding tube Zircaloy-4 $\varnothing_{ext} = 9.50$ mm $t = 0.57$ mm	Cold worked stress relieved state
2	Thimble tube Zircaloy-4 Standard section $\varnothing_{ext} = 12$ mm, $t = 0.40$ mm	Fully annealed state
3	Thimble tube Zircaloy-4 Reduced section $\varnothing_{ext} = 10$ mm, $t = 0.40$ mm	Fully annealed state

As it is known, the statistical error, linked with the number of irradiated grains, varies in

$$1/\sqrt{N_T} \tag{2}$$

This factor 10 increases the error of the density determination by a factor approximately equal to 3. These considerations show that the cross-section of the incident beam must make it possible to irradiate a number of grains, amounting to some hundreds.

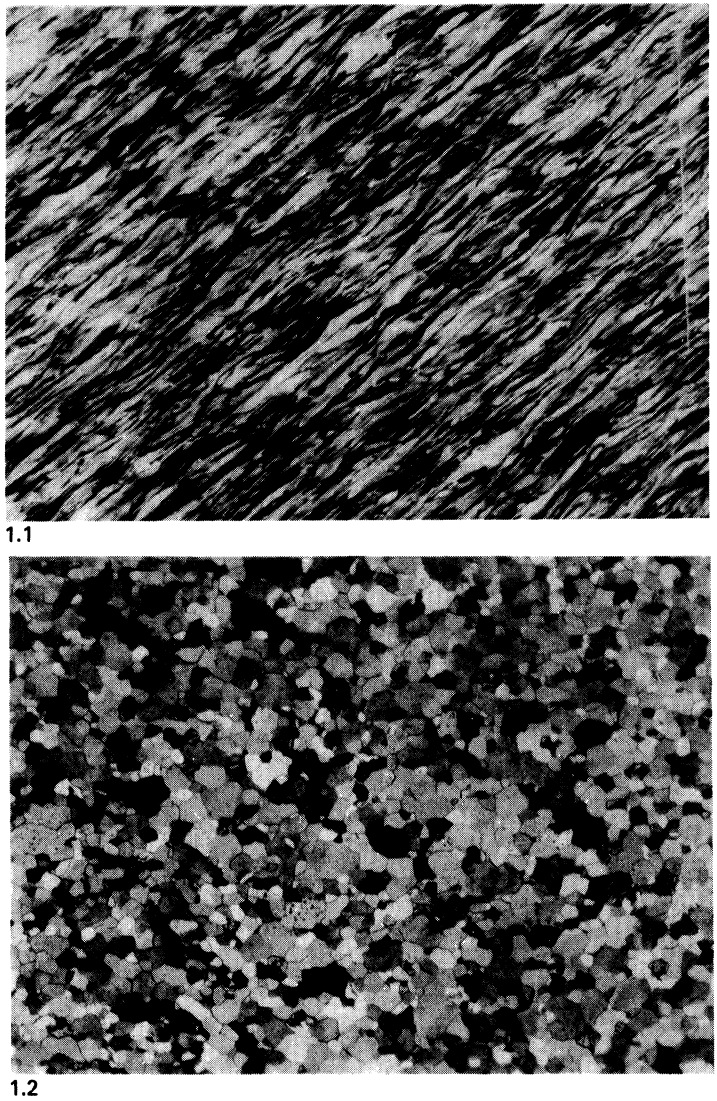

1.1

1.2

Figure 1 Micrographies by ZIRCOTUBE of the different samples of zircaloy-4 (500× magnification). 1.1 cladding tube. 1.2 thimble tube (standard section).

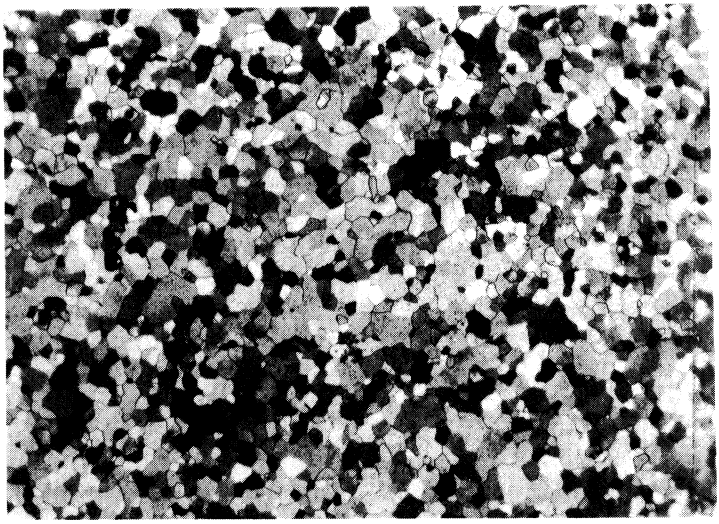

1.3

Figure 1 (*Continued*) 1.3 thimble tube (reduced section).

3. EXPERIMENTAL CONDITIONS OF PFs MEASUREMENT

Only two laboratories have taken into account various samples for each type of product. The other laboratories had to limit their analysis to the detailed examination of one single sample per type of product. This restriction in the number of studied samples does not affect the importance of the results of the "round-robin," all the more as the laboratories, which studied the three samples taken from different parts of the tubes, have observed that the textures of the same product do hardly vary (great homogeneity of the textures).

All laboratories worked with computer controlled texture goniometers and with the K_α line of copper.

They have chosen collimator adjustments on the source side and slits on the side of the counter, except for the LAMM because of the linear detection principle, which made it possible to eliminate the geometrical defocalisation effect beyond 75° of the tilt angle, which is the commonly chosen limit for the measurement of all incomplete pole figures.

On the contrary, the particularities of the adjustments, the amplitudes of the scannings and the detection techniques change from one laboratory to another and are presented in Table 3.

We should bear in mind that in the specifications of the contract, the measurement of PFs (00.2), (10.2), (10.1) plus one of the two PFs (11.0) or (10.2) were planned. However, the laboratories have restricted their reports to the presentation of the PFs as quoted in Table 4.

We are restricting our synthesis to the presentation of PFs (00.2), which were determined by all laboratories.

Table 3 Experimental conditions of PFs measurement in the various laboratories.

	CRU Ugine	*LAMM St Nazaire*	*LECM CEN Grenoble*	*LM2P Metz*	*SRMA CEN Saclay*
Detector	Diode Si–Li	Linear detector opening 11° in 2θ	Scintillation counter	Scintillation counter	Diode Si–Li
Particularity		Simultaneous measure of 3 PFs (10.0), (00.2) and (10.1)	Primary graphite monochromator	Ni Filter	
Tilt angle step	5°	5°	2.5°	2.5°	2.25°
Azimuthal step	1°	7.5°	5°	5°	4°
Type of scan	Step scan	Continuous scan	Continuous scan	Continuous scan	Continuous scan
Time for 1 measure (s)	3	15	5	5	3
Translation (mm)	±5	±6	±4	±3	±3
Collimator (mm)	$\varnothing = 0.3$	$\square = 0.5$	$\varnothing = 0.8$	$\varnothing = 0.5$	$\square = 2 \times 2.8$
Background measurement	yes	yes	yes	yes	yes
Correction of the defocalisation	unnecessary for the chosen adjustments	unnecessary because of the detector	unnecessary for the chosen adjustments	unnecessary for the chosen adjustments	if the case arises

Table 4 Pole figures presented by the different laboratories.

	CRU Ugine	*LAMM St Nazaire*	*LECM CEN Grenoble*	*LM2P Metz*	*SRMA CEN Saclay*
00.2	×	×	×	×	×
10.0	×	×	×	×	×
10.1	×	×		×	×
11.0	×				×
10.2				×	×

4. CORRECTION AND NORMALIZATION OF POLE FIGURES

In the framework of these measurements, various laboratories have chosen experimental conditions so that the estimated influence of the defocalisation phenomenon is eliminated beyond an angle of 75° which is the limit for measurements as stated in the specifications of the contract.

Apart from the subtraction of the background scattering, which is estimated thanks to measurements performed out of Bragg conditions, there is a need to make further corrections in the experimental measurements. The number of pulses registered per time unit by the counter is proportional to the density of lattice planes, which are in the Bragg position. The factor of proportionality is linked to numerous factors, such as the capacity of the installation, the measurement time, the diffraction line, the efficiency of the counter etc.

For complete pole figures, this factor of proportionality or of norm can be easily calculated, as we know the integral of pole figure density on the semi-sphere has to be 2π. *For incomplete pole figures,* this factor can be estimated by measuring the diffraction on samples of isotropic texture while preserving the other experimental conditions. However, the preparation of such samples is very difficult. In order to compare easily the results obtained by the laboratories we have chosen a pseudo-normalization on the portion of the sphere, on which measurements are performed (Kern and Bergmann, 1978).

N_i represents the pseudo-norm:

$$N_i = \frac{2\pi(1 - \cos \alpha_{\max})}{\int_{\alpha=0}^{\alpha_{\max}} \int_{\beta=0}^{2\pi} I_{hi}(\alpha, \beta) \sin \alpha \, d\alpha \, d\beta} \tag{3}$$

where $\alpha_{\max}$ is the maximum of the tilt angle and $I_{hi}(\alpha, \beta)$ the experimental intensity of PFs.

The pseudo-norm can be quite far from the real norm, especially when all poles are inside the portion of the sphere, but it makes it possible to compare results from different origins. The average values of $P_{hi}(\alpha, \beta)$ on solid angles, which are defined by selecting the steps of the tilt angle, the steps of azimuthal scanning as well as the collimators, are the only ones known from the practical point of view. The choice of these steps determines the resolving power on the one hand and the smoothing of the measurement on the other hand.

Hence, the pseudo-norm N_i is likely to vary from one laboratory to another, because of different choices of angular steps of integration, without the possibility of evaluating quantitatively the differences thus introduced when comparing the results. In addition, the variation of the integration steps brings about different smoothings for the "measured" amplitudes of the intensities of the PFs peaks which cannot be expressed in numbers either.

5. RESULTS

5.1. *Experimental Pole Figures*

The first part of the interlaboratories tests is limited to the comparison of the experimental pole figures normed after the pseudo-norm and corrected from the attenuation due to the defocalisation, if there was any (see §4).

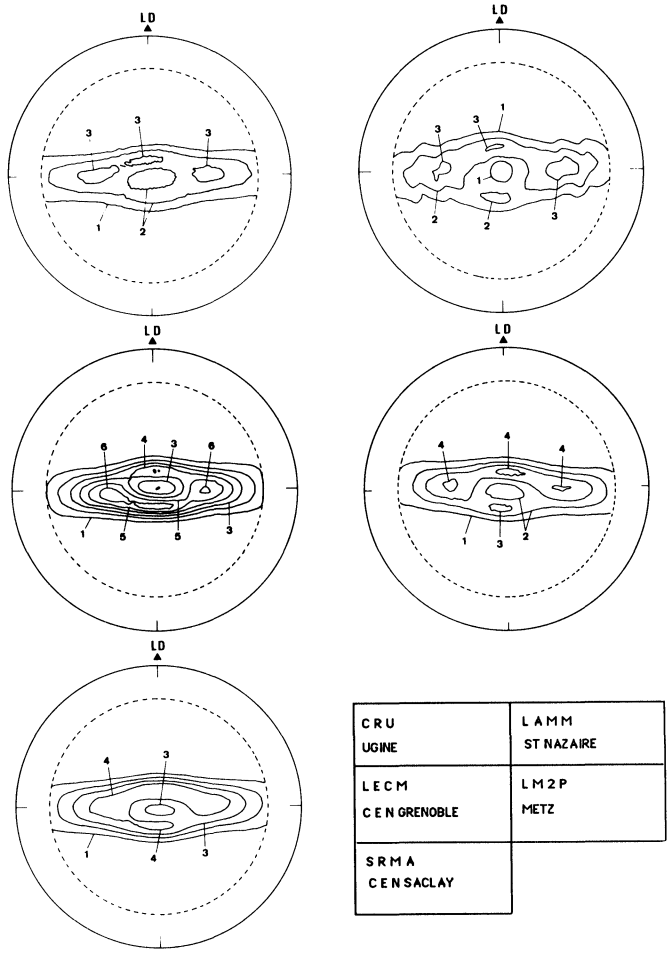

Figure 2.1 Experimental pole figures (0.02) determined by the different laboratories for cladding tubes.

In this sense, the specifications advised a standardization of incomplete pole figure diagrams in a circle of $\phi = 20$ cm for 90° according to a choice of levels, which are entire multiples of the isotropy, the first level 0.5 being optional.

For the first part of the interlaboratories tests, comparisons are only performed on the basis of the qualitative study of PFs diagrams. This study is facilitated by the gathering of the PFs (00.2) on the same plate just as they are obtained by the different laboratories for a sample of the same type, respectively the cladding tube (fig. 2.1), the thimble tube of the standard section (fig. 2.2) and reduced section (fig. 2.3).

The textures of zircaloy tubes and sheets, which have undergone an intense forming process, are strongly marked. Pole figures (00.2) of the basis planes generally present two intense peaks, which are symmetrical according to the

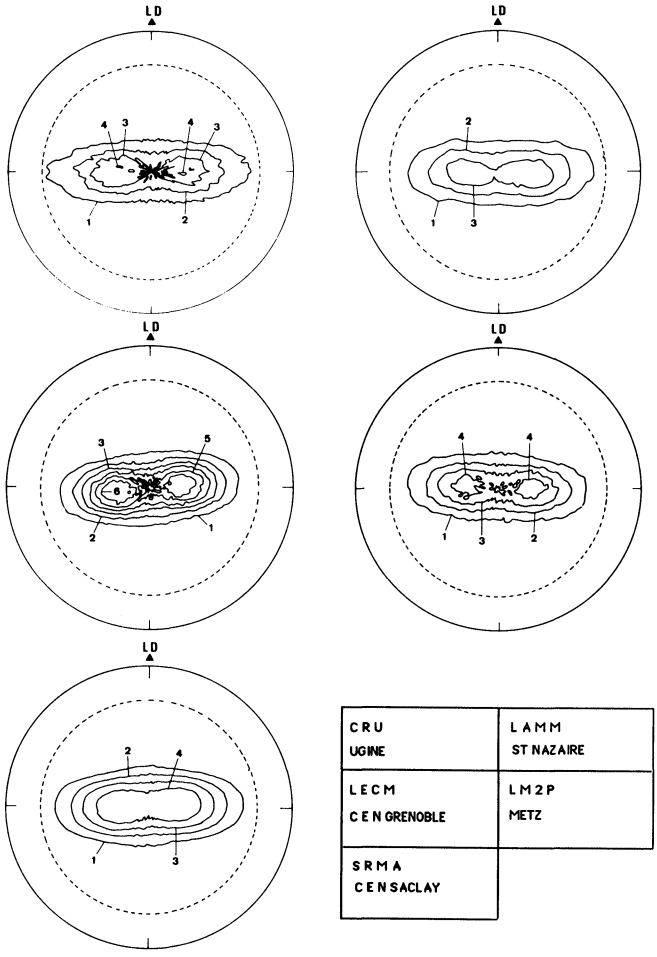

Figure 2.2 Experimental pole figures (00.2) determined by the different laboratories for thimble tube, standard section.

centre of the figure. These textures can be schematically classified according to the location of these two peaks of the PF (00.2) in the texture of the L type (lengthwise poles), of the T type (transversewise poles) or less frequently of the C type (central poles), which can be considered as a limit case of one of the two previous cases when peaks get closer to the centre.

The textures of zircaloy-4 tubular products, studied in these interlaboratories tests are all of the T type as the PFs (00.2) present two pronounced maxima situated in the (RD, TD) plane, which are symmetrical to the centre of the figure.

However, these textures of the T type can be distinguished according to the angular position and the amplitude of their maxima. Moreover, pole figures (00.2) of the three tubular products are dissymmetrical in the (RD, TD) plane.

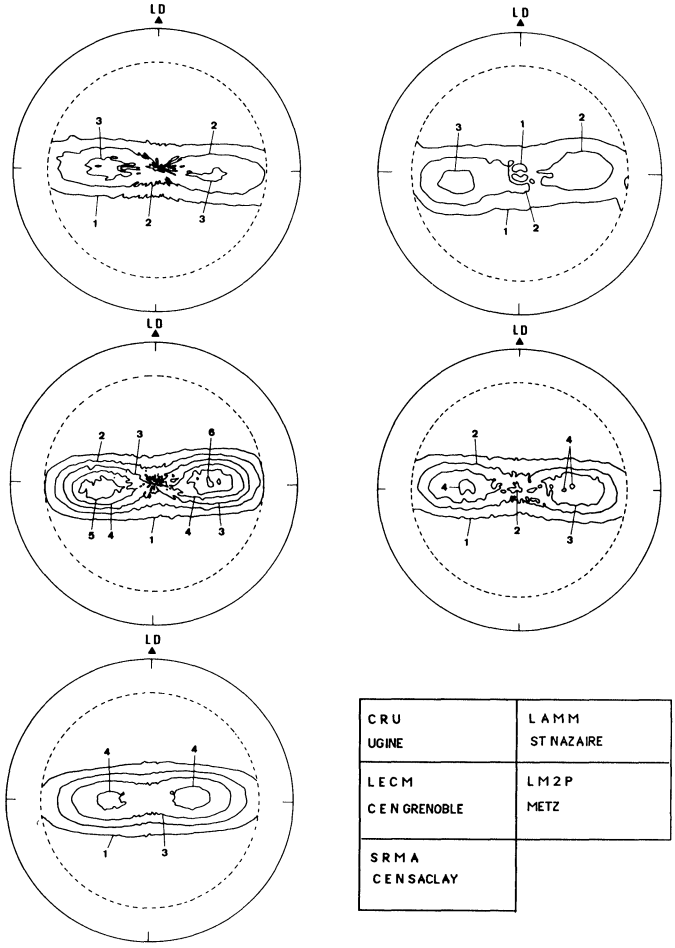

Figure 2.3 Experimental pole figures (00.2) determined by the different laboratories for thimble tube, reduced section.

This fact is noticed thanks to a difference in relation to the symmetry of the orthorhombic sample. This dissymmetry is caused by the pilgrim's step process undergone by the tubes. Thus the maxima of the pole figures (00.2) are not exactly localized in (RD, LD) and (RD, TD) planes. The easiest way to describe these peaks "profiles" is to make linear sections of FPs according to the planes (RD, LD) or (RD, TD) respectively.

5.2. (RD, LD) *and* (RD, TD) *Linear Sections of the Pole Figures* (00.2)

Figures 3 and 4 show the (RD, LD) and (RD, TD) linear sections of the pole figures (00.2) which were obtained for the three types of samples, by the different laboratories. The comparison of these results can only be qualitative as the

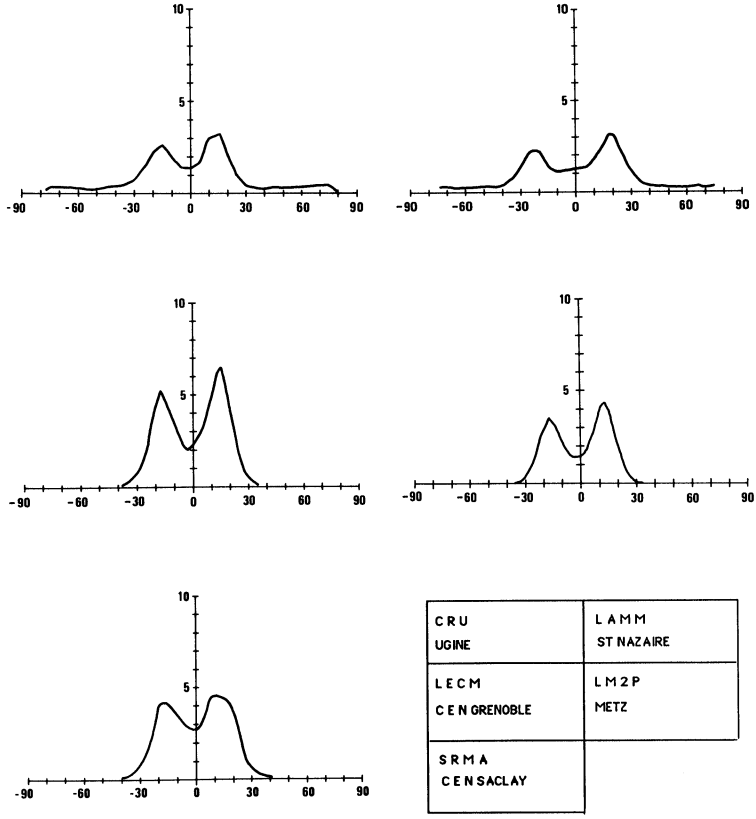

Figure 3 (RD, LD) linear sections of the pole figures (00.2) measured by the different laboratories on cladding tubes.

laboratories used different steps for the tilt angle and different programs for the diagrams, which are more or less smoothed, depending on the technique used. In order to compare the results, the position and amplitudes of the lengthwise and transversewise maxima are represented in Figures 5 and 6 for the cladding tube, the linear sections of which are the most marked ones. From the point of view of the angular position, the results are clearly clustered in length, as the maxima are strongly marked. The scattering is wider in the transverse direction because of the greater spread of the peaks.

5.3. *Calculation of Kearns Coefficients*

The f_R, f_T and f_L Kearns coefficients make it possible to calculate the average properties of hexagonal polycrystals which can be represented by tensors of the second rank such as growth under radiation, thermal dilatation etc. These

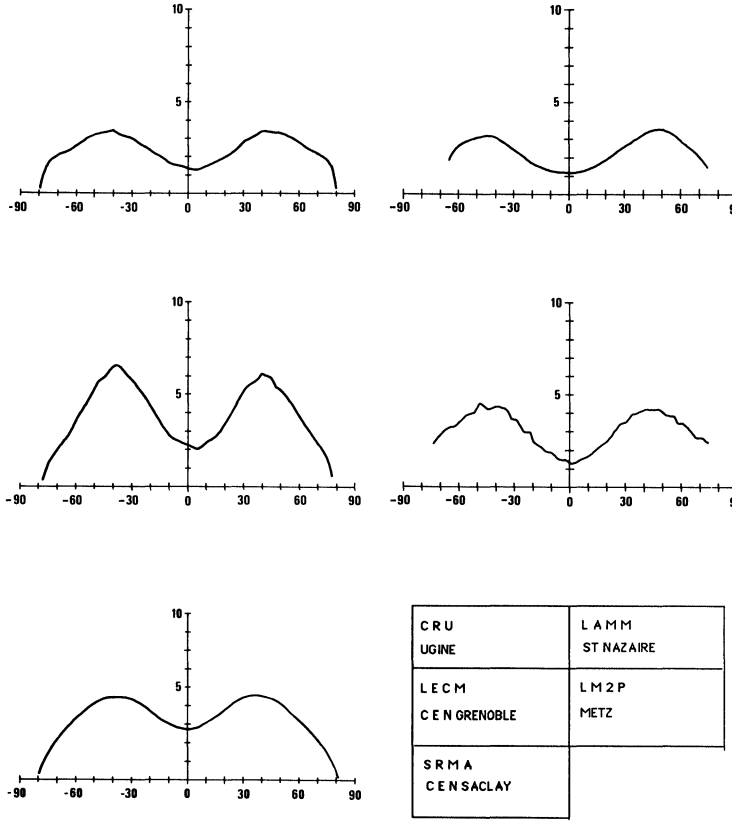

Figure 4 (RD, TD) linear sections of the pole figures (00.2) measured by the different laboratories on cladding tubes.

coefficients are defined by the following integrals:

$$f_i = \frac{1}{2\pi} \int_{\alpha=0}^{2\pi} \int_{\beta=0}^{2\pi} P_{00.1}(\alpha, \beta) \cos^2 \alpha_i \sin \alpha \, d\alpha \, d\beta \tag{4}$$

where $\cos \alpha_i$ are the direction cosines in the macroscopic frame, with α, β as spherical polar coordinates, Figure 7.

As far as the calculation of the pole figure (00.2) is concerned, we notice that virtually all poles are contained in the portion of the sphere, which is defined by the maximum tilt angle of $\alpha_{max} = 75°$. These conditions make it possible to calculate directly the Kearns coefficients and the norm of the PF (00.2) thanks to the incomplete PF (00.2), with a very satisfactory approximation.

$$f_i = \frac{\int_{\alpha=0}^{\alpha_{max}} \int_{\beta=0}^{360°} I_{00.2}(\alpha, \beta) \cos^2 \alpha_i \sin \alpha \, d\alpha \, d\beta}{\int_{\alpha=0}^{\alpha_{max}} \int_{\beta=0}^{360°} I_{00.2}(\alpha, \beta) \sin \alpha \, d\alpha \, d\beta} \tag{5}$$

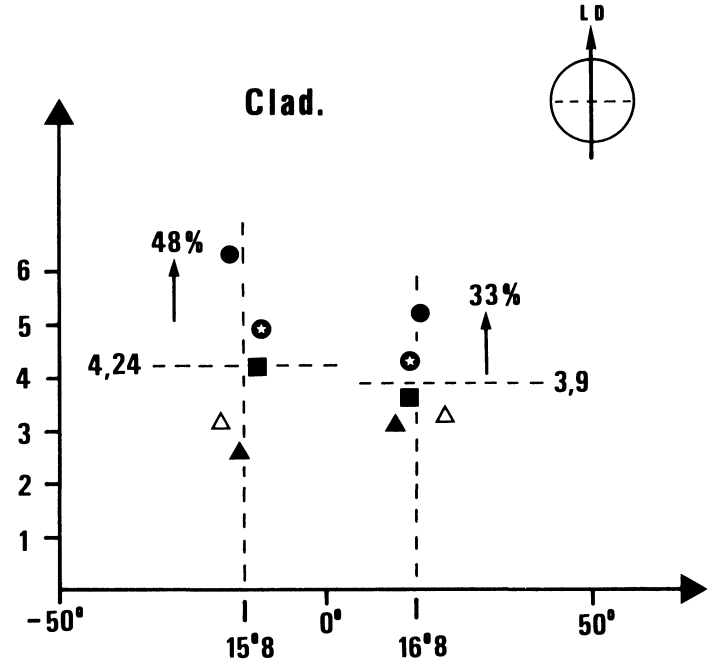

Figure 5 Lengthwise maxima of the (RD, LD) linear sections of the pole figures (00.2) presented by the different laboratories for the cladding tube.

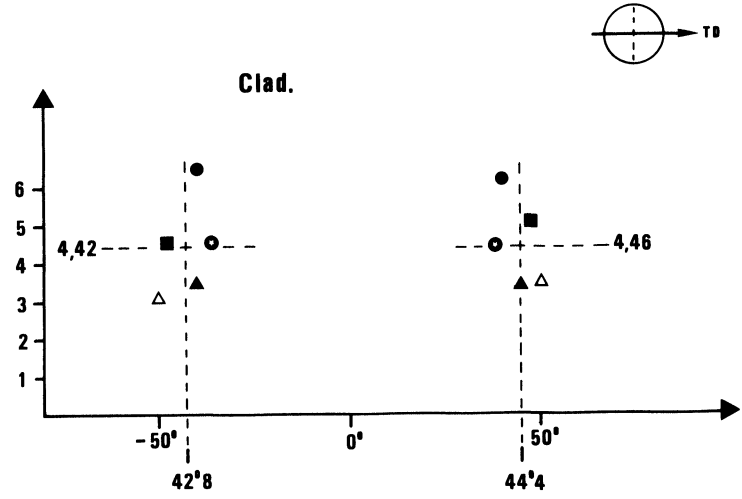

Figure 6 Transversewise maxima of the (RD, TD) linear sections of the pole figures (00.2) presented by the different laboratories for the cladding tube.

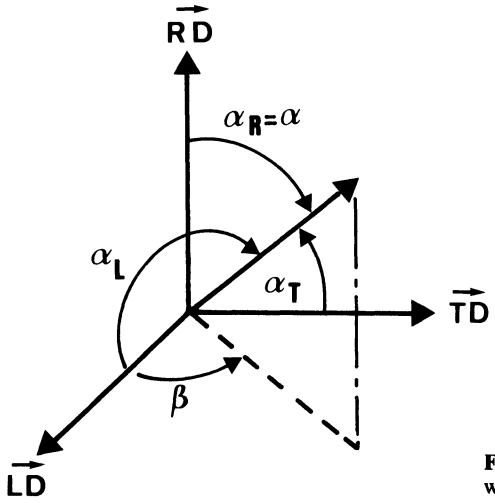

Figure 7 Direction cosines in the sample frame with α, β as the spherical polar coordinates.

Of course, the previous limitating observations concerning the practical calculation and the deviations among the pseudo-norms results of different origins (§4), do all the more apply to the calculation of norms and Kearns coefficients (Table 5).

This table is summarized on the Figure (8), which shows that, on the whole, the results are clustered with fairly low spread for the f_R and f_T coefficients with high values which is true for any samples. The highest spread is observed for the f_L coefficients, which are very low and thus especially sensitive to the evaluation of the background scattering, but, also to the sampling of the sphere of poles (measurement steps), and to the numerical exploitation, as assumed in paragraph 4.

Table 5 Represents Kearns coefficients, which were obtained by the different laboratories for the cladding tube, the thimble tube of the standard and reduced section.

		CRU Ugine	*LAMM St Nazaire*	*LECM Grenoble*	*LM2P Metz*	*SRMA Saclay*
Cladding	f_R	0.590	0.570	0.672	0.630	0.607
	f_T	0.324	0.338		0.329	0.323
	f_L	0.097	0.092		0.039	0.069
Thimble standard	f_R	0.627	0.653	0.721	0.700	0.641
	f_T	0.268	0.261		0.255	0.276
	f_L	0.106	0.082		0.043	0.082
Thimble reduced	f_R	0.558	0.539	0.601	0.592	0.583
	f_T	0.353	0.378		0.361	0.341
	f_L	0.099	0.082		0.045	0.075

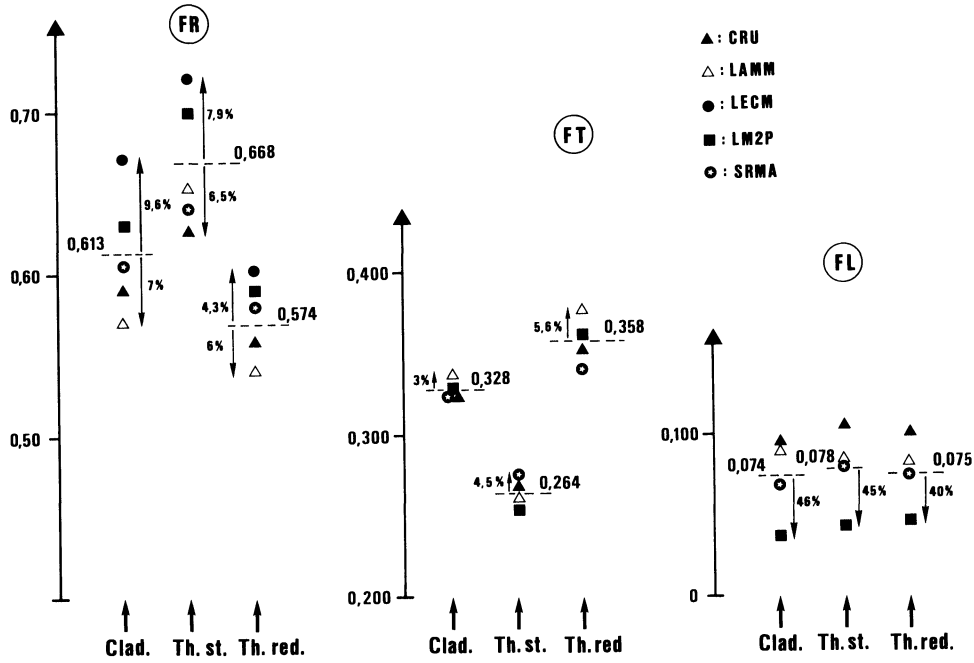

Figure 8 Graphic representation of the Kearns coefficients, gathered in Table 5.

6. CONCLUSION

On the initiative of ZIRCOTUBE, a manufacturer of tubular zircaloy 4 products and FRAGEMA, a designer, several French laboratories, which are competent in the field of crystallographic textures, have compared their know-how in the framework of these interlaboratories tests.

The synthesis of the different presented reports shows that on the whole the results are rather clustered. The difference which nevertheless remains can be attributed to the different preparations of the samples as well as the choice of the adjustments which modify the statistics of the counter and the smoothing of the measurements.

The evolution of the micro-computer controlled goniometer and detector systems on the one hand and, on the other hand, the know-how sharing to which interlaboratories tests contribute, allow the laboratories equipped with such facilities to perform measurements of comparable quality.

The aim of the comparison of the experimental data set in the program of the first part of the interlaboratories tests has thus been achieved in a satisfactory way by the teams contributing to this publication.

Using the presently achieved measurements as a basis of their work, the different laboratories will now start the second part of the tests i.e. the quantitative texture analyses by means of three-dimensional analysis programs,

which are at their disposal for advanced calculation of crystallographic textures and physical average values for textured polycrystals.

Acknowledgement

The authors are indebted to Professor H. Bunge, T.U. Clausthal, for an efficient proof-reading of the text.

References

Bunge, H. (1982) *Texture Analysis in Materials Science,* Butterworth, London.

Bunge, H. and Esling C., Editors (1982). *Quantitative Texture Analysis,* DGM Oberursel/Frankfurt.

Humbert, M. (1986). "Intensity corrections, resolving power and statistical relevance in pole figure measurements" in *Experimental Techniques of Texture Analysis,* Bunge, H., Editor, DGM Oberursel/Frankfurt, 29.

Lewis, J. E., Schoenberger, G. and Adamson, R. B. (1979). Texture Measurement Techniques for Zircaloy Cladding—A Round Robin Study in ASTM—Zirconium in the nuclear industry, 39.

Kern, R. and Bergmann, H. W. (1978). "A simple way for Calculation ODF from incomplete Pole Figures" in Proceedings of the Fifth International Conference Texture of Materials, Gottstein G., Lücke K., Editors, Springer Verlag, Berlin, **1,** 139.

Kearns, J. J. (1965) WAPD—TM 472 Thermal expansion and preferred orientation in Zircaloy.

Vadon A. (1981) Généralisation et optimisation de la méthode vectorielle d'analyse de la texture, Thesis, University of Metz.